Observation of an Excited State in ^{7}He with Unusual Structure

A. A. Korsheninnikov,[1,*] M. S. Golovkov,[1,*] A. Ozawa,[1] E. A. Kuzmin,[2] E. Yu. Nikolskii,[2] K. Yoshida,[1]
B. G. Novatskii,[2] A. A. Ogloblin,[2] I. Tanihata,[1] Z. Fulop,[1,†] K. Kusaka,[1] K. Morimoto,[1] H. Otsu,[1]
H. Petrascu,[1] and F. Tokanai[1]
[1]*RIKEN, Hirosawa 2-1, Wako, Saitama 351-0198, Japan*
[2]*The Kurchatov Institute, Kurchatov sq. 1, 123 182 Moscow, Russia*
(Received 15 December 1998)

The transfer reaction $p(^8\mathrm{He}, d)^7$He has been studied by correlational measurements, and an excited state of ^{7}He was observed ($E^* = 2.9 \pm 0.3$ MeV, $\Gamma = 2.2 \pm 0.3$ MeV) which decays mainly into $3n + {}^4$He. Most likely, it has a structure with a neutron in an excited state coupled to the ^{6}He core which itself is in the excited 2^+ state. [S0031-9007(99)09012-2]

PACS numbers: 25.60.–t, 23.20.En, 27.20.+n, 21.45.+v

We report on such a novel step, in the experiments with beams of exotic nuclei, as the investigation of transfer reactions. Namely, we studied the $p(^8\mathrm{He}, d)^7$He reaction for the spectroscopy of ^{7}He.

It is well known that nuclei have excited states. There is a famous exception from this rule—the absence of excited states in ^{3}He and ^{3}H. Another kind of exception was ^{7}He. This nucleus was investigated for 30 years in many reactions with stable beams, and no excited states were found. As a result, ^{7}He began to be considered as a nucleus which may not have excited states. It can be explained by a large width for decay $^7\mathrm{He}^* \rightarrow n + {}^6$He. The ground state of ^{7}He is a well established resonance that decays into $n + {}^6$He.

Radioactive nuclear beams are the most promising tool to study as neutron-rich systems as ^{7}He. Since the projectiles in reactions are already neutron rich, reaction mechanisms are simpler than those with stable beams, cross sections are higher, and physical backgrounds are lower. We used a beam of ^{8}He at 50*A* MeV, that was produced by the fragment separator RIPS at RIKEN, and studied the $p(^8\mathrm{He}, d)^7$He reaction with the CH_2 and C targets. To study transfer reactions with beams of exotic nuclei, a special detection system, the RIKEN telescope, was designed (Fig. 1). It represents a stack of solid-state position-sensitive detectors (strip detectors) that have large area and annular hole. Using this telescope, we detected deuterons at small angles in the laboratory system (10°–25°) corresponding to a high cross section.

In addition to the deuterons, we detected other particles emitted from the decay of ^{7}He. Neutrons were measured by the neutron walls of plastic scintillators, while charged particles were bent in the dipole magnet and detected by the drift chamber and the plastic scintillators' hodoscope (Fig. 1). These parts of the detection system allowed us to study spectra of deuterons detected in coincidences with ^{6}He, ^{4}He, and neutrons. Other detectors in Fig. 1, the beam scintillators and multiwire proportional counters, were used for identification of each beam particle, determination of its energy, and for its tracking.

The resulting deuteron spectra are presented in Figs. 2 and 3 as a function of energy in the center of mass of ^{7}He relative to the $n + {}^6$He threshold. In each graph, the upper histogram with pronounced peak corresponds to measurements with CH_2 target; the lower structureless histogram shows total background from materials other than protons in the target (it was obtained with the C and empty targets). The cutoff of spectra at energy of ~30 MeV reflects the energy range measured by the deuteron telescope according to its thickness.

Figure 2 shows the inclusive deuteron spectrum and spectra of deuterons detected in coincidences with ^{6}He, ^{4}He, and with both of them. A strong peak in Figs. 2(a), 2(b), and 2(c) represents the ^{7}He ground state. This state is not seen in Fig. 2(d), because $^7\mathrm{He}_{\mathrm{g.s.}}$ cannot decay into ^{4}He ($^7\mathrm{He}_{\mathrm{g.s.}}$ is lower than the $^4\mathrm{He} + 3n$ threshold). Instead, in Fig. 2(d) there is another peak that corresponds to an excited state of ^{7}He. This state is seen in Fig. 2(b) as a peak marked by an arrow. The $^7\mathrm{He}^*$ state can also be seen in Fig. 2(a), if one takes into account that the background has a slope [subtracting the background from the CH_2 histogram, we obtained a spectrum that has a shape similar to that in Fig. 2(b)]. Thus, the ^{7}He excited state is observed in Figs. 2(a), 2(b), and 2(d). However, this state can hardly be distinguished in Fig. 2(c) in coincidences with ^{6}He.

In Fig. 3, spectra of deuterons are presented, which were measured in coincidences with neutrons in addition. Again, the ^{7}He ground state is seen as a strong peak in

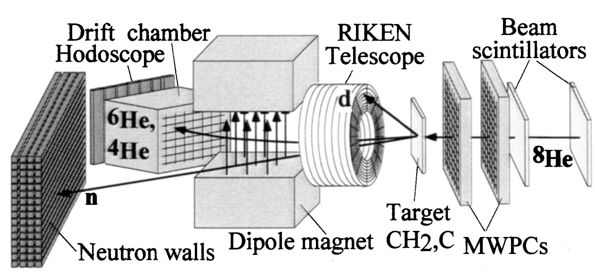

FIG. 1. Schematic of the experimental setup.

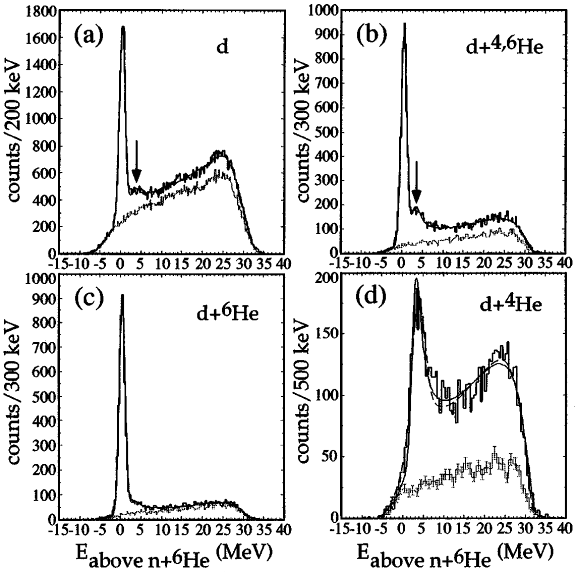

FIG. 2. Spectra of deuterons from reactions: (a) $p(^8\mathrm{He}, d)$; (b) $p(^8\mathrm{He}, d^{4,6}\mathrm{He})$; (c) $p(^8\mathrm{He}, d^6\mathrm{He})$; (d) $p(^8\mathrm{He}, d^4\mathrm{He})$. The spectra are shown as a function of ^{7}He energy above the $n + {}^6$He threshold.

Figs. 3(a), 3(b), and 3(c). In Fig. 3(d), coincidences with ^{4}He exclude the ground-state peak and reveal perfectly the excited state. The latter is also observed in Figs. 3(a) and 3(b) as small peaks marked by arrows. However, in coincidences with ^{6}He in Fig. 3(c), the excited state is not seen. Thus, the found excited state decays mainly into $3n + {}^4$He, while its decay into $n + {}^6$He is suppressed in spite of larger decay energy.

Curves in Figs. 2 and 3, which describe perfectly all experimental distributions, were obtained by a fit of the spectra. For the ^{7}He excited state, the Breit-Wigner formula was used. Both the energy dependent width and $\Gamma =$ const were tried [solid curves in Figs. 2 and 3 and dashed curves in Figs. 2(d) and 3(d), respectively]. These line shapes were folded with a Gaussian function for the experimental resolution (FWHM $= 1.5$ MeV). For the ^{7}He ground state, only a Gaussian was used (width of $^7\mathrm{He}_{\mathrm{g.s.}}$ is small, $\Gamma = 160$ keV). Continuum in the $d + n + {}^6$He channel was modeled using a three-body phase space. Continuum in the $d + 3n + {}^4$He channel was described by a five-body phase space and a three-body phase space for $d + n + {}^6\mathrm{He}^*(2^+)$. To obtain fitting functions, the Monte Carlo simulation of experiment was performed to incorporate the phase spaces with the experimental resolution and detection efficiency (in particular, it allows one to describe the cutoff of spectra at ~ 30 MeV). In the Monte Carlo simulation, angular distributions for the nonresonant continuum were fixed: They were extracted from the experimental data and approximated by an exponential function. Contributions from smooth backgrounds (the lower histograms in Figs. 2 and 3) were approximated by polynomials. Using this procedure, we extracted parameters, energy and width, of the ^{7}He excited state. Considering integral yields for the $^7\mathrm{He}^*$ state obtained from different spectra and taking into account acceptances for the particles measured in coincidences with deuterons, we obtained the $^7\mathrm{He}^*$ decay branching ratio.

To investigate a sensitivity of the results to models used for physical continuums, we considered also the $d + 3n + {}^4$He phase space modulated by the final state interactions of $n + n$ and $n + {}^4$He as well as evaporation from the compound system $^9\mathrm{Li}^*$. Shapes of all backgrounds are illustrated in Fig. 4. In addition, we studied the $3n + {}^4$He continuum populated in fragmentation of ^{8}He, in sudden approximation. The ^{8}He wave function obtained in the $4n + \alpha$ model [1] was used, and the distribution over relative energy in the ^{7}He subsystem was extracted. A shape of this distribution was found to be similar to that of the $3n + {}^4$He phase volume in a wide range of the ^{7}He energy (up to ~ 20 MeV).

As a result, the following parameters of the ^{7}He excited state were obtained: the energy relative to the $n + {}^6$He threshold $E_{\mathrm{obs}} = 3.3 \pm 0.3$ MeV, the excitation energy

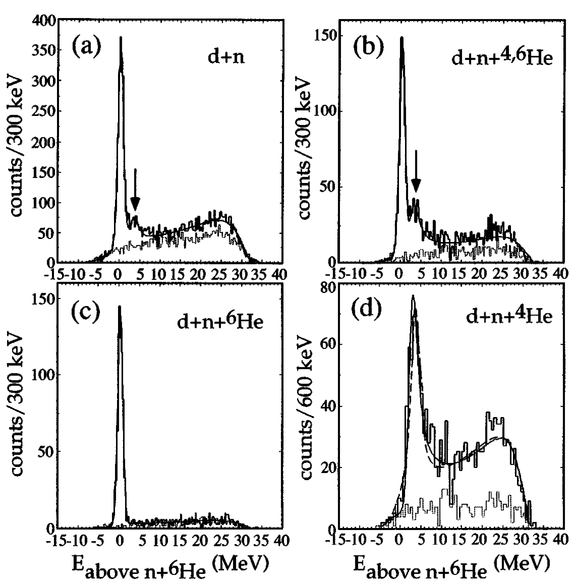

FIG. 3. Spectra of deuterons from reactions: (a) $p(^8\mathrm{He}, dn)$; (b) $p(^8\mathrm{He}, d^{4,6}\mathrm{He})$; (c) $p(^8\mathrm{He}, dn^6\mathrm{He})$; (d) $p(^8\mathrm{He}, dn^4\mathrm{He})$.

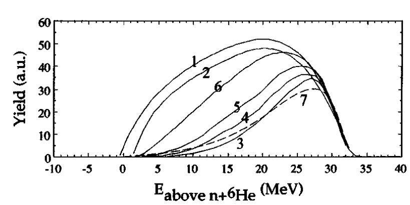

FIG. 4. Physical backgrounds: 1—phase volume (PV) $d + {}^6\mathrm{He} + n$; 2—PV $d + {}^6\mathrm{He}^*(2^+) + n$; 3—PV $d + {}^4\mathrm{He} + 3n$; 4—final state interaction (FSI) $n + n$; 5—FSI $n + {}^4$He; 6—FSI $n + n$ simultaneously with FSI $n + {}^4$He; 7—evaporation from the compound system $^9\mathrm{Li}^*$.

counted from $^7\mathrm{He}_{\mathrm{g.s.}}$ is then $E^* = 2.9 \pm 0.3$ MeV, the width $\Gamma_{\mathrm{obs}} = 2.2 \pm 0.3$ MeV, and the decay branching $\Gamma_{\alpha+3n}/\Gamma_{\mathrm{tot}} = 0.7 \pm 0.2$.

The excitation energy E^* does not contradict a recent paper [2], where the $^9\mathrm{Be}(^{15}\mathrm{N}, ^{17}\mathrm{F})^7\mathrm{He}$ reaction was studied and a peak at $E^* = 3.2$ MeV was observed, which was considered by the authors of Ref. [2] as a "good candidate for the $1/2^-$ resonance of ^{7}He." In Ref. [2], the authors also found an alternative explanation of this peak: It can be described by the sequential decay in flight of $^{18}\mathrm{F}^*$ into $^{17}\mathrm{F} + n$. In our experiment an analogous mechanism would be the sequential decay of excited states of ^{6}Li into $d + {}^4$He. The corresponding calculations showed that in our case the sequential decays are completely irrelevant to the $^7\mathrm{He}^*$ peak, giving a high-energy bump such as curves 3–7 in Fig. 4.

Subdividing the spectra, which were presented above in the overall angular acceptance of the deuteron telescope, into spectra corresponded to narrow angular ranges, we extracted angular distributions for the reactions $^8\mathrm{He}(p,d)^7\mathrm{He}_{\mathrm{g.s.}}$ and $^8\mathrm{He}(p,d)^7\mathrm{He}^*$. At that we confirmed that positions of both peaks, $^7\mathrm{He}_{\mathrm{g.s.}}$ and $^7\mathrm{He}^*$, do not depend on the angle, as it ought to be for the population of a nuclear state. The obtained angular distributions are shown in Fig. 5. The presented cross section for the ^{7}He excited state corresponds to the decay into ^{4}He (thus, it should be divided by the $^7\mathrm{He}^*$ decay branching to obtain the full cross section of the $^7\mathrm{He}^*$ population).

The decay scheme of ^{7}He is shown in Fig. 6. The most interesting finding is that the revealed excited state decays predominantly into $3n + {}^4$He, in spite of a larger $n + {}^6$He decay energy. It reflects an unusual structure of this state. To investigate its detailed structure, we considered the antisymmetrized $3n + \alpha$ wave function and studied three outer neutrons in the $P_{3/2}$ and $P_{1/2}$ orbitals relative to the α core as well as in the $P_{3/2}$ and $S_{1/2}$ orbitals. The configuration $(P_{3/2})^2(P_{1/2})^1$ can produce excited states of ^{7}He with $J^\pi = 1/2^-, 3/2^-$, and $5/2^-$. The configuration $(P_{3/2})^1(P_{1/2})^2$ gives $J^\pi = 3/2^-$. Combinations of $P_{3/2}$ and $S_{1/2}$ orbitals correspond to $J^\pi = 1/2^+, 3/2^+, 5/2^+$, and $3/2^-$. Below, we discuss possible assignments for the spin parity of the ^{7}He excited state.

$1/2^-$: The $^7\mathrm{He}^*(1/2^-)$ wave function contains the ^{6}He subsystem produced by the $(P_{3/2})^2$ pair of neutrons with a norm of $P(0^+) = 100\%$. Thus, $^7\mathrm{He}^*(1/2^-)$ has to decay mainly into $n + {}^6\mathrm{He}_{\mathrm{g.s.}}$, and this is in contradiction with the experimental results. So, this configuration does not correspond to the observed $^7\mathrm{He}^*$ state. In addition, a width for the decay $^7\mathrm{He}^*(1/2^-) \to n + {}^6\mathrm{He}_{\mathrm{g.s.}}$, which was evaluated using the R-matrix formula $\Gamma_{\mathrm{obs}} = 2P\gamma^2/(1 + \gamma^2 dS/dE)$ [3] with the channel radius taken in a broad range of $R_c = 2.5$–6 fm, occurs to be larger ($\sim$5 MeV) than the experimental width of $^7\mathrm{He}^*$ ($\sim$2 MeV).

$3/2^-$: The $(P_{3/2})^2(P_{1/2})^1$ configuration in $^7\mathrm{He}^*(3/2^-)$ contains the ^{6}He subsystem produced by $(P_{3/2})^2$ with a norm of $P(2^+) = 100\%$. The $^6\mathrm{He}(0^+)$ subsystem does not exist either in the $(P_{3/2})^2$ or in the $(P_{3/2})^1(P_{1/2})^1$ pair of neutrons. Thus, this configuration should mainly decay into $n + {}^6\mathrm{He}^*(2^+)$. This configuration should be mixed with the $(P_{3/2})^1(P_{1/2})^2$ configuration which also does not contain the $^6\mathrm{He}_{\mathrm{g.s.}}$ subsystem and should decay into $n + {}^6\mathrm{He}^*(2^+)$. The $(P_{3/2})^1(S_{1/2})^2$ configuration does not decay either into $^6\mathrm{He}_{\mathrm{g.s.}}$ or into $^6\mathrm{He}^*(2^+)$; it should be mixed with the above discussed configurations, making a width of $^7\mathrm{He}^*(3/2^-)$ narrower.

$5/2^-$: The $^7\mathrm{He}^*(5/2^-)$ wave function does not contain the $^6\mathrm{He}(0^+)$ subsystem and has the $^6\mathrm{He}(2^+)$ subsystem produced by $(P_{3/2})^2$ with $P(2^+) = 100\%$. It should decay into $n + {}^6\mathrm{He}^*(2^+)$.

$1/2^+, 3/2^+, 5/2^+$: These states are inconsistent with the experimental observations, because they should have very broad widths due to an absence of centrifugal barrier ($L = 0$) for decays into $n + {}^6\mathrm{He}_{\mathrm{g.s.}}$ (for $J^\pi = 1/2^+$) and into $n + {}^6\mathrm{He}^*(2^+)$ (for $3/2^+$ and $5/2^+$).

As a result, two candidates, $^7\mathrm{He}^*(3/2^-)$ and $^7\mathrm{He}^*(5/2^-)$, attract attention. $^7\mathrm{He}^*(3/2^-)$ should decay mainly into $n + {}^6\mathrm{He}^*(2^+)$ with the subsequent decay $^6\mathrm{He}^* \to 2n + {}^4$He. It is consistent with the experimental observation of $^7\mathrm{He}^*$ decay into $3n + {}^4$He. Moreover, the R-matrix calculations reproduce the experimental width and decay branching. The latter corresponds to a small weight ($\leq$10%) of the $^6\mathrm{He}(0^+)$ subsystem in $^7\mathrm{He}^*(3/2^-)$,

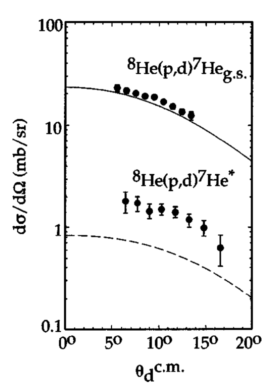

FIG. 5. Angular distributions for the reactions $^8\mathrm{He}(p,d)^7\mathrm{He}_{\mathrm{g.s.}}$ and $^8\mathrm{He}(p,d)^7\mathrm{He}^*$.

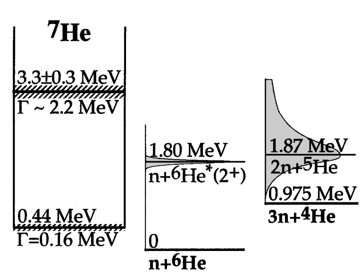

FIG. 6. Decay scheme of ^{7}He.

which is what is expected for an admixture of the second order. However, in spite of such a self-consistency and agreement with the experiment, there is an argument against the $3/2^-$ interpretation of the observed state. In Ref. [4], the resonating group method was applied to investigate ^{7}He as a particle unstable state. In particular, a phase shift was calculated for scattering of $n + {}^6\text{He}^*(2^+)$ in $3/2^-$ channel. This phase shift does not show any resonance. Resonantlike structures were found only for $5/2^-$ scattering of $n + {}^6\text{He}^*(2^+)$ and $1/2^-$ scattering of $n + {}^6\text{He}_{\text{g.s.}}$ with broader width.

The $^7\text{He}^*(5/2^-)$ state should also decay into $n + {}^6\text{He}^*(2^+)$ with the subsequent decay $^6\text{He}^* \rightarrow 2n + {}^4\text{He}$. The experimental width can be reproduced by the R-matrix calculations. As it was mentioned, the $5/2^-$ phase shift of the $n + {}^6\text{He}^*(2^+)$ scattering shows a resonancelike structure [4]. These facts are in favor of the $5/2^-$ interpretation of the observed state. However, in the frame of R-matrix theory it is impossible to explain the experimental decay branching by the second order admixtures of the $n + {}^6\text{He}(0^+)$ configuration. A large centrifugal barrier ($L = 3$) for the decay into $n + {}^6\text{He}_{\text{g.s.}}$ makes the $n + {}^6\text{He}^*(2^+)$ decay dominant with practically 100% branching. The $5/2^-$ interpretation becomes consistent with the experiment, if the observed $^6\text{He}_{\text{g.s.}}$ fraction, that was included in the decay branching, in reality has no relation to the $^7\text{He}^*_{3.3}$ state, but appeared due to, e.g., a broad state $^7\text{He}^*(1/2^-)$.

We do not discuss here configurations with $D_{5/2}$ orbitals, because their phase shifts calculated in Ref. [4] do not show a resonant behavior. At last, we considered the decays of $^7\text{He}^*$ into $3n + {}^4\text{He}$ via $^6\text{He}^*(2^+)$, while the direct decay into $3n + {}^4\text{He}$ was neglected as well as decays via the broad state of ^{5}He (Fig. 6) or via the singlet state of ^2n. Partial widths of those decays should be strongly suppressed by a phase-volume factor due to a larger number of particles than that for $n + {}^6\text{He}^*(2^+)$ (the width of $^6\text{He}^*$ is very narrow, 113 keV, so this decay can be considered as a two-particle process).

Thus, a structure of the revealed $^7\text{He}^*$ level should represent a neutron in an excited state coupled to the ^{6}He core which itself is in the excited 2^+ state. It is consistent with a structure of ^{8}He used as a projectile. It was noticed [5], that the ground state of ^{8}He contains mainly the ^{6}He subsystem in the excited 2^+ state. Indeed, considering the antisymmetrized ^{8}He wave function in the $4n + \alpha$ model with four neutrons in the $P_{3/2}$ orbital relative to the α core, we obtained the following norms for various J^π in the ^{6}He subsystem: $P(0^+) = 17\%$, $P(1^+) = 0$, $P(2^+) = 83\%$, $P(3^+) = 0$.

Finally, we discuss the cross sections in Fig. 5. The reaction $p(^8\text{He}, d)^7\text{He}_{\text{g.s.}}$ corresponds to pickup of the valence neutron from ^{8}He. As mentioned above, ^{8}He is specific with respect to the ^{6}He subsystem. However, we found that the antisymmetrized $3n + \alpha$ wave function of $^7\text{He}_{\text{g.s.}}$ with neutrons in $P_{3/2}$ orbitals relative to the α core has the same norms for various J^π of the ^{6}He subsystem [$P(0^+) = 17\%$, $P(2^+) = 83\%$] as that in ^{8}He. Thus, the $p(^8\text{He}, d)^7\text{He}_{\text{g.s.}}$ reaction should have a large cross section. The solid curve in Fig. 5 shows the distorted-wave Born approximation calculation without any fit to the experimental data. The optical potential parameters for $p, d + {}^{12}\text{C}$ scattering at close energy [6] were used, the spectroscopic factor was equal to 4 (four valence neutrons in ^{8}He); the $n + {}^7\text{He}$ potential was chosen to reproduce the radius of the valence neutron in ^{8}He, $R_v = 3.1$ fm [1].

The $p(^8\text{He}, d)^7\text{He}^*$ reaction has a lower cross section because it is the second order process: In addition to the pickup of a neutron from ^{8}He, another neutron should occur in the excited state [while the $^6\text{He}(2^+)$ core is already "prepared" in ^{8}He]. For the case of $^7\text{He}^*(5/2^-)$, this reaction can go via a small admixture of $P_{1/2}$ orbital in ^{8}He. Its weight is unknown, and for rough estimation the $P_{1/2}$ weight in ^{6}He ($\sim$4%) was used, which we extracted from the ^{6}He wave function calculated in Ref. [7]. The dashed curve in Fig. 5 shows the calculated cross section for $p(^8\text{He}, d)^7\text{He}^*(5/2^-)$. It describes well a shape of the experimental data, while absolute values indicate that the two-step process, which involves a neutron excitation in addition to the neutron pickup, should be important also.

In summary, in correlational measurements of the nucleon transfer reaction with an exotic ^{8}He beam, we have observed the excited state of ^{7}He at 3.3 ± 0.3 MeV above the $n + {}^6\text{He}$ threshold with $\Gamma = 2.2 \pm 0.3$ MeV. It decays mainly into $3n + {}^4\text{He}$ in spite of larger $n + {}^6\text{He}$ decay energy. Most likely, this state has a structure with a neutron in the $P_{1/2}$ state coupled to the ^{6}He core which itself is in the excited 2^+ state. Tentative spin assignment for this state is $J^\pi = 5/2^-$.

We are grateful to Professor M. V. Zhukov for critical reading of the paper.

*On leave from Kurchatov Institute, Moscow, Russia.
†On leave from ATOMKI, Debrecen, Hungary.

[1] M. V. Zhukov, A. A. Korsheninnikov, and M. H. Smedberg, Phys. Rev. C **50**, R1 (1994).
[2] H. G. Bohlen *et al.*, in *Proceedings of the VI International School-Seminar on Heavy Ion Physics, Dubna, Russia, 1997*, edited by Yu. Ts. Oganessian and R. Kelpakchieva (World Scientific, Singapore, 1998), p. 134.
[3] A. Lane and R. Thomas, Rev. Mod. Phys. **30**, 257 (1958).
[4] J. Wurzer and H. M. Hofmann, Phys. Rev. C **55**, 688 (1997).
[5] M. V. Zhukov (private communication).
[6] K. Hatanaka *et al.*, Nucl. Phys. **A419**, 530 (1984).
[7] B. V. Danilin, M. V. Zhukov, A. A. Korsheninnikov, L. V. Chulkov, and V. D. Efros, Sov. J. Nucl. Phys. **53**, 71 (1991).